Fusion Codes of the NRV

(Brief description of the models used)

1. Single-Barrier Penetration Model

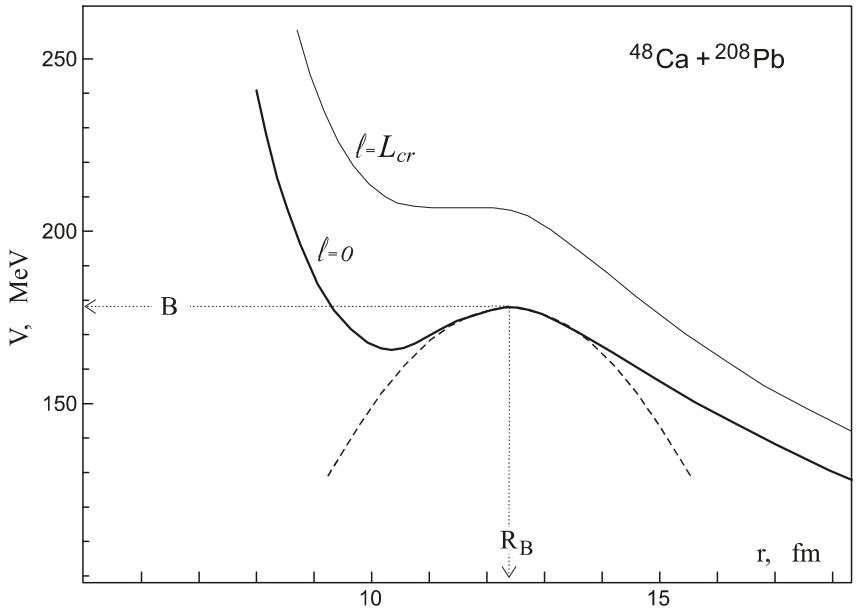

Figure 1 Interaction of two spherical nuclei ^{48}Ca+^{208}Pb. The proximity potential is used here for the nuclear interaction (r_0=1.16 fm, b=1.0 fm). Dashed curve shows the parabolic approximation of the Coulomb barrier. For the partial wave l=L_{cr} (thin solid line) the potential pocket disappears.

Interaction of two nuclei (consisting of the repulsive long-range Coulomb term and attractive short-range nuclear component) reveals a maximum, which is referred to as the Coulomb barrier, see Fig. 1. Position of this maximum (R_B) is usually larger by 1 or 2 fm than the sum of nuclear radii R_1+R_2. At low near-barrier energies the light and/or medium colliding nuclei having overcome the Coulomb barrier and coming in contact are captured in the potential

pocket and fuse (form a compound mono-nucleus). The fusion cross section can be decomposed over partial waves

$$\sigma_{fus}(E) = \frac{\pi\hbar^2}{2\mu E}\sum_{l=0}^{\infty}(2l+1)T_l(E), \tag{1}$$

where μ is the reduced mass of the system, E is the center-of-mass energy, and $T_l(E)$ is the partial barrier transmission probabilities. Within the "**single-barrier penetration model**" transmission probabilities $T_l(E)$ can be calculated by solving one-dimensional Schrödinger equation with appropriate (non-reflective) boundary condition. Approximating the radial dependence of the barrier by a parabola one can use the simple Hill-Wheeler formula [1] for the transmission probabilities

$$T_l^{HW}(B;E) = \left[1+\exp\left(\frac{2\pi}{\hbar\omega_B(l)}\left[B+\frac{\hbar^2}{2\mu R_B^2(l)}l(l+1)-E\right]\right)\right]^{-1}. \tag{2}$$

Here $\hbar\omega_B = \sqrt{\hbar^2/\mu\left|\partial^2 V/\partial r^2\right|_B}$ is defined by the width of the potential barrier, B is the height of the barrier and $R_B(l)$ is the position of the effective barrier including a centrifugal term. Better agreement with experimental data on sub-barrier fusion cross section can be obtained if energy dependence of the barrier width, $\hbar\omega_B(E)$, is taken into account (See Fig. 1).

2. Interaction of Deformed and Deformable Nuclei [2]

The shape of axially deformed nucleus is defined as follows

$$R(\vec{\beta},\theta) = \tilde{R}\cdot\left(1+\sum_{\lambda\geq 2}\beta_\lambda\sqrt{\frac{2\lambda+1}{4\pi}}P_\lambda(\cos\theta)\right), \tag{3}$$

where $\vec{\beta}\equiv\{\beta_\lambda\}$ are dimensionless deformation parameters of multi-polarity $\lambda = 2,3,\ldots$, P_λ are the Legendre polynomials,

$$\tilde{R} = R_0\left[1+\frac{3}{4\pi}\sum_\lambda\beta_\lambda^2+\frac{1}{4\pi}\sum_{\lambda,\lambda',\lambda''}\sqrt{\frac{(2\lambda'+1)(2\lambda''+1)}{4\pi(2\lambda+1)}}(\lambda'0\lambda''0\,|\,\lambda0)^2\beta_\lambda\beta_{\lambda'}\beta_{\lambda''}\right]^{-1/3} \tag{4}$$

R_0 is the radius of equivalent sphere of the same volume, and $(\lambda'0\lambda''0\,|\,\lambda0)$ are the Clebsh-Gordan coefficients. Potential energy of two deformable nuclei is the sum of the Coulomb, nuclear, and deformation energies

$$V_{12}(r;\vec{\beta}_1,\theta_1,\vec{\beta}_2,\theta_2) = V_C(r;\vec{\beta}_1,\theta_1,\vec{\beta}_2,\theta_2)+V_N(r;\vec{\beta}_1,\theta_1,\vec{\beta}_2,\theta_2)+\frac{1}{2}\sum_{i=1}^{2}\sum_\lambda C_{i\lambda}\cdot\left(\beta_{i\lambda}-\beta_{i\lambda}^{g.s.}\right)^2. \tag{5}$$

Here and below the index *i = 1,2* numerates the nuclei, $C_{i\lambda}$ are the surface stiffness parameters, and $\theta_{1,2}$ are the orientations of symmetry axes, see Fig.2.

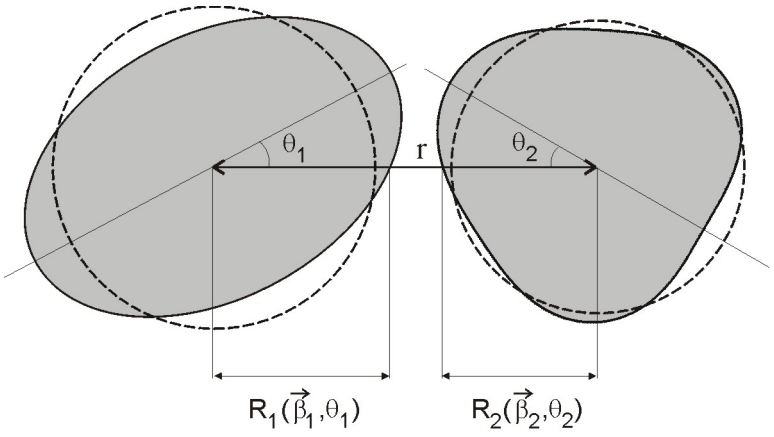

Figure 2 Schematic picture of two deformed nuclei rotating in the reaction plane.

The Coulomb interaction of two deformed nuclei is given by

$$V_C = Z_1 Z_2 e^2 \left[F^{(0)}(r) + \sum_{i=1}^{2} \sum_{\lambda \geq 2} F_{i\lambda}^{(1)}(r) \beta_{i\lambda} Y_{\lambda 0}(\theta_i) \right] + Z_1 Z_2 e^2 \sum_{i=1}^{2} \sum_{\lambda'} \sum_{\lambda''} \sum_{\lambda=|\lambda'-\lambda''|}^{\lambda=\lambda'+\lambda''} F_{i\lambda}^{(2)}(r) \sum_{\mu} \int Y_{\lambda'\mu}^{*} \, Y_{\lambda''-\mu}^{*} \, Y_{\lambda 0} d\Omega \cdot \beta_{i\lambda'} \beta_{i\lambda''} Y_{\lambda 0}(\theta_i) + \ldots \quad (6)$$

At $r > R_1 + R_2$, $F^{(0)} = \frac{1}{r}$, $F_{i\lambda}^{(1)} = \frac{3}{2\lambda+1} \frac{R_i^{\lambda}}{r^{\lambda+1}}$, $F_{i\lambda=2}^{(2)} = \frac{6}{5} \frac{R_i^2}{r^3}$, $F_{i\lambda=4}^{(2)} = \frac{R_i^4}{r^5}$. At shorter values of *r*, when nuclear surfaces overlap, there are more complicated expressions for the form-factors $F_{\lambda}^{(n)}(r)$. It is not important here because $R_C^B > R_1 + R_2$. Usually nuclei have quadrupole and hexadecapole static deformations ($\lambda = 2, 4$).

The short-range nuclear interaction depends on a distance between nuclear surfaces $\xi = r - R_1(\vec{\beta}_1, \theta_1) - R_2(\vec{\beta}_2, \theta_2)$, see Fig. 2. The Woods-Saxon potential is often used to describe this interaction:

$$V_{WS}(\xi) = \frac{V_0}{1 + \exp(\zeta / a)},$$

where $\zeta = r - R_V - \Delta R_1 - \Delta R_2$, $\Delta R_1 = R_1(\vec{\beta}_1, \theta_1) - R_1$, and $\Delta R_2 = R_2(\vec{\beta}_2, \theta_2) - R_2$. Note, that for the Woods-Saxon potential the interaction radius $R_V = r_0^V (A_1^{1/3} + A_2^{1/3})$ does not usually coincide with a sum of nuclear radii, and r_0^V is an additional independent parameter. "Proximity" potential is an another choice for parameterization of the nucleus-nucleus interaction [3]

$$V_{prox}(\xi) = 4\pi\gamma b P_{sph}^{-1} \cdot \Phi(\xi / b) \quad (7)$$

here $\Phi(\xi / b)$ is universal dimensionless form-factor, b is the thickness parameter of nuclear surface ($\approx$1fm), $\gamma = \gamma_0(1 - 1.7826 \cdot I^2)$, $\gamma_0 = 0.95\,\mathrm{MeV \cdot fm^{-2}}$ is the surface stiffness, $I = (N - Z)/A$, $\xi = r - R_1(\vec{\beta}_1, \theta_1) - R_2(\vec{\beta}_2, \theta_2)$, and $P_{sph} = 1/\bar{R}_1 + 1/\bar{R}_2$, where $\bar{R}_i = R_i[1 - (b/R_i)^2]$. This interaction is very sensitive to a choice of nuclear matter radii. We can recommended to use the following approximation of this parameter: $r_0(A) = 1.16 + 16/A^2$ for A>14 and $r_0 \approx 1.25$ for $A \leq 14$. An absence of fitting parameters (such as V_0, r_0^V, a_V) is the main advantage of the "proximity" potential.

Attraction of two nuclear surfaces depends also on their curvatures. For deformed nuclei P_{sph} in (7) should be replaced by

$$P\left(\vec{\beta}_1,\theta_1,\vec{\beta}_2,\theta_2\right)=\left[\left(k_1^{\|}+k_2^{\|}\right)\left(k_1^{\perp}+k_2^{\perp}\right)\right]^{1/2} \tag{8}$$

where $k_i^{\|,\perp}$ are the principal local curvatures of the projectile and target. For spherical nuclei $k_i^{\|,\perp}=R_i^{-1}$ and $P=P_{sph}$. At the deformations along inter-nuclear axis ($\theta_1=\theta_2=0$) the local curvature may be found in analytical form [2] and

$$P\left(\vec{\beta}_1,\theta_1=0,\vec{\beta}_2,\theta_2=0\right)=\sum_{i=1,2}\frac{1}{\tilde{R}_i}\left(1+\sum_{\lambda\geq 2}\sqrt{\frac{2\lambda+1}{4\pi}}\beta_{i\lambda}\right)^{-2}\left(1+\sum_{\lambda\geq 2}\left(1+\eta(\lambda)\right)\sqrt{\frac{2\lambda+1}{4\pi}}\beta_{i\lambda}\right) \tag{9}$$

where $\eta(\lambda)=3\cdot 4\cdot\ldots\cdot(\lambda+1)/(\lambda-1)!$. For rotated nuclei one has to distinguish the shortest distance between surfaces ξ_S from the distance along central line - ξ (see Fig. 2). However, for realistic deformations this effect is not so large comparing with a change of surface curvatures in resulting nucleus-nucleus interaction and fusion cross section.

The expression (8) may nominally reduce to zero at some negative deformations (touch of two planes). This non-physical effect originates due to neglecting the finite areas of the touching surfaces. Interactions of nearly located nucleons give the main contribution to the nucleus-nucleus potential energy. The number of such nucleons depends on the surface curvatures but it is always finite. Thus, instead of a simple replacement of P_{sph} by P in (7), the expression $V_N=G(\vec{\beta}_1,\theta_1,\vec{\beta}_2,\theta_2)\cdot V_N^0(r,\vec{\beta}_1,\theta_1,\vec{\beta}_2,\theta_2)$ is more appropriate, where V_N^0 is the nucleus-nucleus interaction calculated ignoring a change in surface curvatures and $G(\vec{\beta}_1,\theta_1,\vec{\beta}_2,\theta_2)$ is the geometrical factor, which takes into account a change in the number of interacted nucleons (located in the nearest layers of two nuclei) comparing with spherical surfaces. The geometrical factor $G(\vec{\beta}_1,\theta_1,\vec{\beta}_2,\theta_2)$ plays important role at large deformations [2].

The stiffness parameters C_λ could be calculated as follows [2]

$$C_\lambda=(2\lambda+1)\frac{\varepsilon_\lambda}{2<\beta_\lambda^0>^2}, \tag{10}$$

here $\varepsilon_\lambda=\hbar\omega_\lambda$ is the vibration energy, $<\beta_\lambda^0>=\frac{4\pi}{3ZR_0^\lambda}\left[\frac{B(E\lambda)}{e^2}\right]^{1/2}$ is the rms deformation of zero vibrations. If there are no experimental data on properties of surface vibration for a given nucleus, then the liquid drop model (LDM) may be used [4]:

$$C_\lambda^{LD}=\gamma_0R_0^2(\lambda-1)(\lambda+2)-\frac{3}{2\pi}\frac{Ze^2}{R_0}\frac{(\lambda-1)}{(2\lambda+1)}, \tag{11}$$

$$D_\lambda^{LD}=\frac{3}{4\pi}\frac{Am_NR_0^2}{\lambda},\qquad \varepsilon_\lambda=\hbar\sqrt{\frac{C_\lambda^{LD}}{D_\lambda^{LD}}}. \tag{12}$$

Here D_λ^{LD} is the mass parameter, A is the mass number, and m_N is the nucleon mass. Note that the liquid drop model sometimes (in particular, for magic nuclei) gives the parameters of surface vibrations, which differ greatly from experimental ones. If the absolute values of nuclear deformations $s_\lambda=\sqrt{\frac{2\lambda+1}{4\pi}}R_0\cdot\beta_\lambda$ are used, the potential energy of surface vibration is written as

$\frac{1}{2}c_\lambda s_\lambda^2$, where $c_\lambda = C_\lambda \cdot \left(\frac{2\lambda+1}{4\pi}R_0^2\right)^{-1} = \frac{\hbar\omega_\lambda}{2 < s_\lambda^0 >^2}$, $< s_\lambda^0 >= \frac{R_0}{\sqrt{4\pi}} < \beta_\lambda^0 >$, and inertia parameter is defined from $\hbar\omega_\lambda = \sqrt{\frac{c_\lambda}{d_\lambda}}$. Within the LDM $d_\lambda^{LD} = D_\lambda^{LD} \cdot \left(\frac{2\lambda+1}{4\pi}R_0^2\right)^{-1} = \frac{3}{\lambda(2\lambda+1)}Am_N$.

3. Driving Potentials

It is clear from (5) that the nucleus-nucleus interaction is a multi-dimensional potential energy surface. If several degrees of freedom (including nucleon transfer, i.e. a change of mass asymmetry) are taken into account with subsequent consideration of the evolution of the nuclear system in multi-dimensional space, then the corresponding potential energy surface, which regulates this evolution, is usually called "driving potential". In. Fig. 3a the two-dimensional interaction potential of spherical nucleus ^{16}O with statically deformed nucleus ^{154}Sm ($\beta_2^{g.s.} = 0.3, \beta_4^{g.s.} = 0.1$) is shown depending on orientation of the last one. In Fig. 3b the potential energy of two initially spherical nuclei ^{40}Ca and ^{90}Zr is shown depending on their dynamic quadrupole deformation (for simplicity it is assumed here that the deformation energies of the two nuclei are proportional to their masses and, instead of two deformation parameters β_1 and β_2, only one $\beta = \beta_1 + \beta_2$ is used). In the first case the Woods-Saxon potential is used with $V_0 = -105$ MeV, $r_0^V = 1.12$ fm, and $a_V = 0.75$ fm. In the second case the "proximity" potential is used with $r_0^i = 1.16$ fm for nuclear radii. The plots demonstrate the multi-dimensional character of the nucleus-nucleus interaction and of potential barrier (compare with Fig. 1). As can be seen, it is impossible to characterize the potential barrier by a specific value *B* of its height. Instead there is some continuous barrier distribution $F(B)$. In fusion process of very heavy nuclei the mass asymmetry degree of freedom (nucleon exchange) plays very important role [5]. The corresponding driving potential can be also calculated using the formula (5) up to the contact point ($r \geq R_1 + R_2$). It may be plotted then, for example, in the (r, η)-space, where $\eta = (A_1 - A_2)/(A_1 + A_2)$ is the mass asymmetry. At shorter distances (overlapped nuclei) additional physics assumptions should be attracted to calculate the potential energy [5].

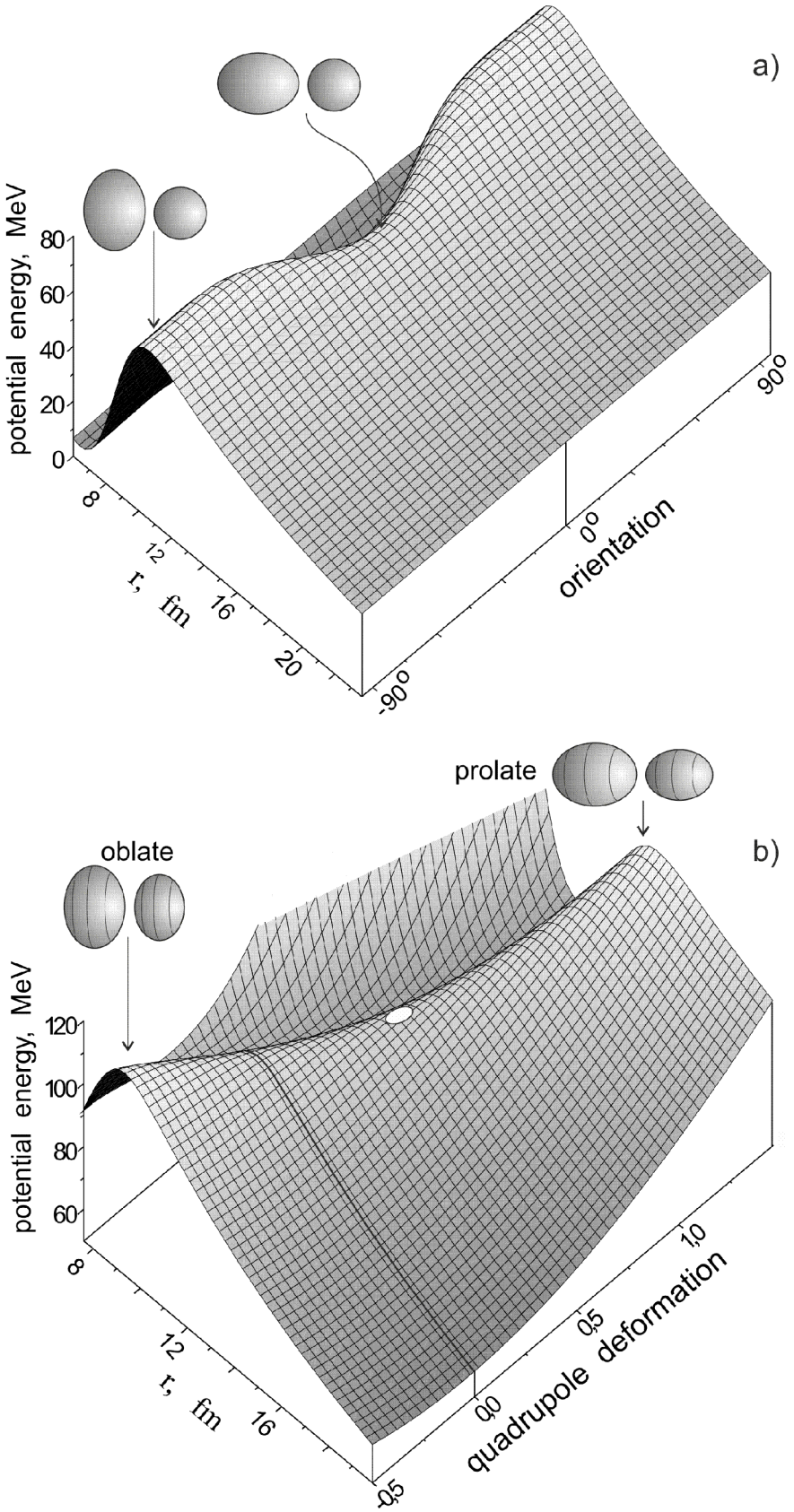

Figure 3 (a) Potential energy of ^{16}O and ^{154}Sm ($\beta_2^{g.s.} = 0.3, \beta_4^{g.s.} = 0.1$) depending on a distance between two nuclei and their mutual orientation. (b) Potential energy surface of the ^{40}Ca + ^{90}Zr interaction depending on quadrupole dynamic deformations of two nuclei. The minimal value of the fusion barrier (saddle point) is marked by the open circle.

4. Empirical Channel Coupling Model

The resent very precise experiments on near-barrier fusion reactions give a possibility to determine rather accurately the second derivative of $E\sigma_{fus}(E)$, which in classical limit may be identified with the so called "barrier distribution function" [6] .

$$D(B) = \frac{1}{\pi R_B^2} d^2(E\sigma_{fus}) / dE^2 \,|_{E=B} \tag{13}$$

The structure of the function $D(B)$ (different for different pairs of nuclei) was found testifying to complicated dynamics of penetration of the potential barrier taking place in strong channel coupling condition.

Penetrability of one-dimensional barrier is defined by the well-known Hill-Wheeler formula (2). In that case the penetration probability $T_l(B,E)$ depends not arbitrary on B and l, but it is a function of the argument $x = B + \frac{\hbar^2}{2\mu R_B^2} l(l+1) - E$, i.e., $T_l(B;E) = f(x)$. Using expression (1) for the fusion cross section, one may write

$$\frac{d\left(E\sigma_{fus}\right)}{dE} = \frac{\pi\hbar^2}{2\mu} \sum_{l=0}^{\infty} (2l+1) \frac{dT_l\left(B;E\right)}{dE} . \tag{14}$$

Because

$$\frac{dT}{dE} = -\frac{dT}{dx} = -\frac{dT}{dl}\left(\frac{dx}{dl}\right)^{-1} = -\frac{dT}{dl}\frac{2\mu R_B^2}{\hbar^2}\frac{1}{2l+1},$$

then

$$\frac{d(E\sigma_{fus})}{dE} = -\pi R_B^2 \sum_{l=0}^{\infty} \frac{dT_l(B;E)}{dl} .$$

In collision of heavy nuclei many partial waves contribute to the fusion cross section, $T_l(B;E)$ is a smooth function of l, and summation in (14) may be replaced by the integration over l. This integral can be easily calculated giving $d(E\sigma_{fus}) / dE = \pi R_B^2 \cdot T_{l=0}(B;E)$, or

$$D(E) = \frac{1}{\pi R_B^2} \frac{d^2(E\sigma_{fus})}{dE^2} = \frac{dT_{l=0}(B;E)}{dE} \tag{15}$$

In classical limit $T(E) = 1$ at $E > B$ and $T(E) = 0$ at $E < B$, i.e., $D(E) = \delta(E - B)$. In quantum case the penetration probability is given by (2) and the function $D(E)$ has one maximum at $E = B$ with the width $\hbar\omega_B \ln(17 + 12\sqrt{2}) / 2\pi \approx 0.56\hbar\omega_B$ (for parabolic barrier).

In real case the nucleus-nucleus potential energy is a multi-dimensional surface (see Fig. 3) and the incoming flux overcomes the Coulomb barrier at different values of its height B (different values of dynamic deformations and/or orientations). In [5] the **semi-empirical channel coupling model** has been proposed for a simple estimation of multi-dimensional barrier penetrability basing on the idea of the "barrier distribution function". There are two cases: (i) fusion reactions involving spherical nuclei and (ii) reactions with statically deformed nuclei.

1. Coupling to vibrational states (fusion of spherical nuclei)

Near-barrier fusion of spherical nuclei strongly depends on coupling of their relative motion to surface vibrations. In this case the Coulomb barrier depends on dynamic deformations. The total penetration probability should be averaged over barrier height B, and instead of (2) one may write

$$T_l(E) = \int F(B)\, T_l^{HW}\left[B(\beta); E\right] dB, \tag{16}$$

where the normalized function $F(B)$ may be approximated by symmetric Gaussian

$$F(B) = N \cdot \exp\left(-\left[\frac{B - B_0}{\Delta_B}\right]^2\right) \tag{17}$$

located at $B_0 = (B_1 + B_2)/2$ and having the width $\Delta_B = (B_2 - B_1)/2$. The value of quantity B_1 corresponds to minimal value of the two-dimensional barrier depended on dynamic deformation (saddle point in Fig. 3b), and B_2 defined as the Coulomb barrier of spherical nuclei. For very heavy nuclei, when the difference $(B_2 - B_1)$ is rather large (greater than 10 MeV), an asymmetric Gaussian with slightly less "inner" width ($\Delta_B^1 \le \Delta_B^2$) approximates better the function $F(B)$ [5].

2. Coupling to rotational states (fusion of statically deformed nuclei)

For statically deformed nuclei the penetration probability should be averaged over the orientations of both nuclei (see Fig. 3a). In this case the total penetration probability is given by

$$T_l(E) = \frac{1}{4}\int_0^{\pi}\int_0^{\pi} T_l^{HW}\left[B\left(\vec{\beta}_1, \theta_1, \vec{\beta}_2, \theta_2\right); E\right] \sin\theta_1 \sin\theta_2 d\theta_1\, d\theta_2, \tag{18}$$

where $B(\vec{\beta}_1, \theta_1; \vec{\beta}_2, \theta_2)$ is the orientation dependent barrier (see Fig. 3a), $\vec{\beta}_1$ and $\vec{\beta}_2$ are the static deformation parameters of interacting nuclei.

3. Coupling to vibrational and rotational states (fusion of spherical and statically deformed nuclei)

The interaction of the spherical nucleus (e.g., projectile) and the statically deformed nucleus (e.g., target) is schematically shown in Figure 4a. Figure 4b shows the dependence of the Coulomb barrier height on the dynamic deformation of the projectile calculated for three different orientations of the target. It is seen, that the curves shift approximately by the same value when the orientation of the target changes.

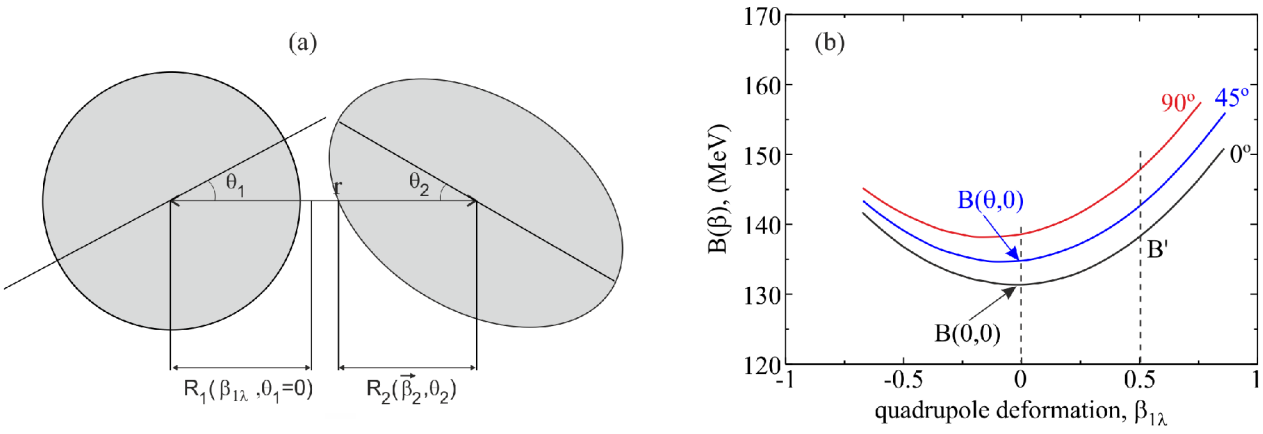

Figure 4 a) Schematic picture of spherical and statically deformed nuclei in the reaction plane. b) Potential energy as a function of dynamic deformation for three different angles of orientation (θ_2) of target.

Thus, one may parametrize the barrier B for the arbitrary value of the projectile deformation (β) and target orientation (θ) as follows:

$$B(\theta,\beta) = B' + \left[B\left(\theta,0\right) - B\left(0,0\right) \right], \quad B' = B(0,\beta). \tag{19}$$

For spherical projectile and statically deformed target the penetration probability should be averaged over the deformation-dependent barrier height as well as the orientations of both nuclei. Then the total penetration probability is given by

$$T_l(E) = \frac{1}{2}\int_0^{\pi} \sin\theta_2 \, d\theta_2 \int F(B') T_l^{HW}\left[B(\theta,\beta); E \right] dB'. \tag{20}$$

5. Neutron Transfer in Fusion Reactions [7]

Recently it becomes clear that intermediate neutron transfer (in fact, this process should be named "neutron rearrangement") plays also an important role for some specific pairs of fusing nuclei, namely for neutron transfer with positive Q-values. It is very difficult, for many reasons, to take into account explicitly the transfer channels within the consistent channel coupling approach (see below) used successfully for the description of collective excitations in the near-barrier fusion processes. However numerical solution of the time-dependent Schrödinger equation [8] clear demonstrates that spreading of the valence neutron's wave function into the volume of the other nucleus takes place before touching of these nuclei and before the colliding nuclei overcome the Coulomb barrier. Among other things this supports the idea of "sequential fusion" mechanism proposed in [7].

In [7] the semi-empirical model was proposed which allows one to include the coupling to the neutron rearrangement channels in the fusion dynamics. It is evident that the incoming flux may penetrate the multidimensional Coulomb barrier in the channels with different intermediate neutron rearrangement. In contrast with neutrons, due to the Coulomb repulsion, rearrangement of protons may occur only after overlapping of colliding nuclei, i.e., after overcoming the Coulomb barrier. Thus the proton transfer should play a minor role in fusion dynamics. Denote by $\alpha_k(E,l,Q)$ the probability for the transfer of k neutrons at the center-of-mass energy E and relative motion angular momentum l in the entrance channel to the final state with $Q < Q_0(k)$, where $Q_0(k)$ is a Q-value for the ground state to ground state transfer reaction. Neutron transfer probability is calculated as follows

$$\alpha_k\left(E,l,Q\right) = N_k \exp\left(-CQ^2\right) \exp\left(-2\kappa\left[d\left(E,l\right) - d_0\right]\right) \tag{21}$$

where $\kappa = \kappa(\varepsilon_1) + \kappa(\varepsilon_2) + ... + \kappa(\varepsilon_k)$ for sequential transfer of k neutrons, $\kappa(\varepsilon_i) = \sqrt{2\mu_n \varepsilon_i / \hbar^2}$ and ε_i is the separation energy of the i-th transferred neutron, $d\left(E,l\right)$ is the distance of the closest approach along the Coulomb trajectory with angular momentum l, $d_0 = R_1^{(n)} + R_2^{(n)} + 2\,fm$ is a parameter, $R_1^{(n)}$ and $R_2^{(n)}$ are the orbit radii of the valence (transferred) neutrons of colliding nuclei (adjusted parameters), and

$$N_k = \left[\int_{-E}^{Q_0(k)} \exp\left(-C\left[Q - Q_{opt} \right]^2 \right) dQ \right]^{-1}$$

is the normalization constant.

The total penetration probability (which takes into account the rearrangement of neutrons with positive Q-value) can be calculated by formulas (16) or (18) in which $T_l^{HW}\left[B;E\right]$ has to be replaced by the following expression

$$\tilde{T}_l^{HW}\left[B;E\right] = \frac{1}{N_{tr}} \sum_k \int_{-E}^{Q_0(k)} \alpha_k\left(E,l,Q\right) \cdot T_l^{HW}\left[B;E+Q\right] dQ, \tag{22}$$

where $N_{tr} = \sum_k \int \alpha_k\left(E,l,Q\right) dQ$ is the normalization constant and $\alpha_0 = \delta\left(Q\right)$.

Note, that simultaneous transfer of two neutrons might be enhanced by factor $N_{2n} \sim 3$ as compared to independent (subsequent) transfer of these neutrons (see, for example, [9]).

6. Channel Coupling Approach [2,10]

Hamiltonian of two deformable nuclei rotating in reaction plane is written as

$$H = -\frac{\hbar^2 \nabla_r^2}{2\mu} + V_C\left(r;\vec{\beta}_1,\theta_1,\vec{\beta}_2,\theta_2\right) + V_N\left(r;\vec{\beta}_1,\theta_1,\vec{\beta}_2,\theta_2\right) + \sum_{i=1,2}\frac{\hbar^2 \hat{I}_i^2}{2\Im_i} + \sum_{i=1,2}\sum_{\lambda\geq 2}\left(-\frac{1}{2d_{i\lambda}}\frac{\partial^2}{\partial s_{i\lambda}^2} + \frac{1}{2}c_{i\lambda}s_{i\lambda}^2\right) \quad (23)$$

where $\Im_i$ are the moments of inertia. Decomposing the total wave function over the partial waves

$$\Psi_{\vec{\mathbf{k}}}(r,\vartheta,\vec{\alpha}) = \frac{1}{kr}\sum_{l=0}^{\infty} i^l e^{i\sigma_l}(2l+1)\chi_l(r,\vec{\alpha})P_l(\cos\vartheta) \quad (24)$$

one get the following set of the coupled Schrödinger equations

$$\frac{\partial^2}{\partial r^2}\chi_l(r,\vec{\alpha}) - \frac{l(l+1)}{r^2}\chi_l(r,\vec{\alpha}) + \frac{2\mu}{\hbar^2}\left[E - V(r,\vec{\alpha}) - \hat{H}_{\text{int}}(\vec{\alpha})\right]\chi_l(r,\vec{\alpha}) = 0 \quad (25)$$

Here $\vec{\alpha}$ are the internal degrees of freedom (deformations and/or angles of rotation)), $H_{\text{int}}(\vec{\alpha})$ is the corresponding Hamiltonian, and $V(r,\vec{\alpha}) = V_C(r,\vec{\alpha}) + V_N(r,\vec{\alpha})$. The functions $\chi_l(r,\vec{\alpha})$ may be also decomposed over the complete set of the eigenfunctions of the Hamiltonian $H_{\text{int}}(\vec{\alpha})$

$$\chi_l(r,\vec{\alpha}) = \sum_{\nu} y_{l,\nu}(r)\cdot\varphi_\nu(\vec{\alpha}) \quad (26)$$

and the radial wave functions $y_{l,\nu}(r)$ satisfy a set of differential equations solved numerically

$$y''_{l,\nu} - \frac{l(l+1)}{r^2}y_{l,\nu} + \frac{2\mu}{\hbar^2}\left[E_\nu - V_{\nu\nu}(r)\right]y_{l,\nu} - \sum_{\mu\neq\nu}\frac{2\mu}{\hbar^2}V_{\nu\mu}(r)y_{l,\mu} = 0 \quad (27)$$

Here $E_\nu = E - \varepsilon_\nu$, ε_ν is the nucleus excitation energy in the channel ν, and $V_{\nu\mu}(r) = <\varphi_\nu | V(r,\vec{\alpha}) | \varphi_\mu>$ is the coupling matrix.

At low energies, not so heavy colliding nuclei having overcome the Coulomb barrier and coming in contact fuse (i.e., form a compound mono-nucleus) with a probability close to unity. The fusion cross section can be measured in that case by detecting all the fission fragments and evaporation residues. Thus, formulating the boundary conditions for the wave function $\Psi_{\vec{\mathbf{k}}}(r,\vartheta,\vec{\alpha})$, it is usually assumed that the flux, which overcomes the Coulomb barrier, is absorbed completely (forming the compound nucleus) and is not reflected from the inner region. It means that at $r < R_{fus} \approx R_1 + R_2$ the functions $\chi_l(r,\vec{\alpha})$ are incoming waves and have not outgoing components reflected from the region $0 \leq r \leq R_{fus}$. The details of satisfying this boundary condition can be found in [2].

At large distances ($r \to \infty$) the wave function has an ordinary behavior of scattering wave: incoming and outgoing waves in the elastic channel $\nu = 0$, and outgoing waves in all other channels. For the partial wave functions this corresponds to the condition

$$y_{l,\nu}(r\to\infty) = \frac{i}{2}\left[h_l^{(-)}(\eta_\nu,k_\nu r)\cdot\delta_{\nu 0} - \left(\frac{k_0}{k_\nu}\right)^{1/2} S_{\nu 0}^l \cdot h_l^{(+)}(\eta_\nu,k_\nu r)\right] \quad (28)$$

where $k_\nu^2 = \frac{2\mu}{\hbar^2}E_\nu$, $\eta_\nu = \frac{k_\nu Z_1 Z_2 e^2}{2E_\nu}$ is the Sommerfeld parameter, $\sigma_{l,\nu} = \arg\Gamma(l+1+i\eta_\nu)$ is the Coulomb partial phase shift, $h_l^{(\pm)}(\eta_\nu,k_\nu r)$ are the Coulomb partial wave functions with the asymptotic behavior $exp(\pm i x_{l,\nu})$, $x_{l,\nu} = k_\nu r - \eta_\nu \ln 2k_\nu r + \sigma_{l,\nu} - l\pi/2$, $S_{\nu 0}^l$ are the partial scattering

matrix elements. Similar expression is obtained for the closed channels ($E_\nu < 0$) with imaginary argument of the function $h_l^{(+)}(\eta_\nu, k_\nu r)$.

The fusion cross section calculated within CC approach is defined by the same expression (1), where the partial transmission coefficients are defined by the ratio of the passed (absorbed) and incoming flaxes

$$T_l(E) = \sum_\nu \frac{j_{l,\nu}}{j_0}. \tag{29}$$

Here

$$j_{l,\nu} = -i\frac{\hbar}{2\mu}(y_{l,\nu}\frac{dy^*_{l,\nu}}{dr} - y^*_{l,\nu}\frac{dy_{l,\nu}}{dr})\Big|_{r\le R_{fus}}$$

is the partial flux in the channel ν, and $j_0 = \hbar k_0 / \mu$.

In the CC Fusion code of the NRV a new effective algebraic method is used for numerical solution of a set of coupled Shrödinger equations [2]. This method has no limitation on the number of coupled channels and allows one to calculate fusion cross sections of very heavy nuclei used for synthesis of super-heavy elements. A combined analysis of the multi-dimensional potential energy surface relief and behavior of the multi-channel wave function in the vicinity of the Coulomb barrier gives a clear interpretation of near-barrier fusion dynamics.

In contrast to light and medium mass nuclei, in fusion of very heavy ions the probability of the compound nucleus (CN) formation after touching of two nuclei is less than unity due to the quasi-fission processes. Calculation of this probability is rather difficult [5] and cannot be performed within the models considered here. For such systems the cross section (1) corresponds to the so-called “capture cross section”, which is equal to a sum of fusion (formation of CN) and quasi-fission (without formation of CN) cross sections.

The cross section of compound nucleus (CN) formation in collisions of heavy nuclei can be calculated as follows

$$\sigma_{fus}^{CN} = \frac{\pi\hbar^2}{2\mu E}\sum_{l=0}^{\infty}(2l+1)T_l(E)\cdot P_{CN}(E,l), \tag{30}$$

where P_{CN} is the probability for CN formation by two nuclei coming in contact. For specific nuclear combinations leading to so called “cold” synthesis a simple parameterization of $P_{CN}(E,l)$ was proposed in [11]

$$P_{CN}(E,l) = \frac{P_{CN}^0(Z_1,Z_2)}{1+\exp\left(\dfrac{E_B^* - E_{\text{int}}^*(l)}{\Delta}\right)}. \tag{31}$$

Here E_B^* is the excitation energy of CN at the Bass barrier and $E_{\text{int}}^*(l) = E + Q - E_{rot}(l)$, where Q is the fusion Q-value, $E_{rot}(l) = \dfrac{\hbar^2}{2\Im_{g.s.}} l(l+1)$ is the rotational energy and

$$P_{CN}^0 = \frac{1}{1+\exp\left(\dfrac{Z_1Z_2 - \varsigma}{\tau}\right)}, \tag{32}$$

where $\varsigma \approx 1760$ and $\tau \approx 45$.

7. Numerical estimation of experimental barrier distribution function [12, 13]

The barrier distribution function $D(E) = \left(\pi R_B^2\right)^{-1}\tilde{D}(E)$, where $\tilde{D}(E) = d^2\left(E\sigma_{\text{fus}}\right)/dE^2$ is not an experimentally measurable quantity but a result of numerical differentiation of

experimental fusion cross sections. Its determination suffers a lot from the limited number of energy values as well as the experimental uncertainties of the cross section measurements. Therefore, the "experimental"' function $\mathrm{D(E)}$ should be better called "estimation of the barrier distribution function" since it cannot be determined unambiguously. To obtain $D(E)$, we use a mathematically correct procedure of two-stage spline smoothing [12,13]. In the initial stage the smoothing spline function $f(E)=\ln\big(F(E)\big)$, $F(E)=E\sigma_{\mathrm{fus}}(E)$ is found from the condition of the minimum of the functional [14]

$$\Phi_1\big[f(E)\big]=\int_{E_0}^{E_n}\big[f''(E)\big]^2dE+\sum_{k=0}^{n}p_k^{-1}\big[f(E_k)-f_k\big]^2, \tag{33}$$

with the experimental values $f_k=\ln\big(E_k\cdot\sigma_{\mathrm{fus,k}}\big)$. The values p_k give a balance between deviation from the values $\mathrm{f_k}$ and smoothness of the approximation and should somehow be determined. It is reasonable to assume that for the points defined with a smaller experimental uncertainty, the approximating curve should pass closer to the points (smaller p_k values), while for the points with larger relative uncertainty, the curve should be smoother (larger p_k). Thus, we approximate p_k by the relative experimental uncertainty of the measured cross section, i.e.,

$$p_k=\frac{\Delta\sigma_{\mathrm{fus}}}{\sigma_{\mathrm{fus}}}. \tag{34}$$

The barrier distribution function values

$$\tilde{D}_k=F''(E_k)=g'(E_k)\exp\big(g(E_k)\big) \tag{35}$$

and estimations of their errors

$$\delta\tilde{D}_k=\left|g'(E_k)\exp\big(g(E_k)\big)-g_0'(E_k)\exp\big(g_0(E_k)\big)\right| \tag{36}$$

are calculated at the second stage by the smoothing function

$$g(E)=\ln F'(E)=f(E)+\frac{1}{2}\ln\big(f'(E)\big)^2, \tag{37}$$

which is found from the condition of the minimum of the functional analogous to (33)

$$\Phi_2\big[g(E)\big]=\int_{E_0}^{E_n}\big[g''(E)\big]^2dE+\sum_{k=0}^{m}q_k^{-1}\big[g(E_k)-g_k\big]^2. \tag{38}$$

The rough blunders are eliminated from the $\mathrm{g_k}$ values, $k=1,\ldots m$. The value of $\mathrm{g_k}$ is considered as a rough blunder if it does not belong to the confidence interval for five neighboring g_i values, where $i=k-2,\ldots k+2$. The q_k values are taken as $q_k=p_k+0.1$.

The function $g_0(E)$ in Eq. (36) is the result of calculation without smoothing, i.e., at the limit $p_k\to 0$.

8. References

[1] D.L. Hill, J.A. Wheeler, Phys.Rev., **89** (1953) 1102.
[2] V.I. Zagrebaev and V.V. Samarin, Yad. Fiz., **67**, No.8 (2004) 1488. [Physics of Atomic Nuclei, 67, No.8 (2004) 1462].
[3] J. Blocki, J. Randrup, W.J. Swiatecki, C.F. Tsang, Ann.Phys.(N.Y.), **105** (1977) 427.
[4] A. Bohr, B.R. Mottelson, Nuclear structure, W.A.Benjamin inc., Amsterdam, 1969.
[5] V.I. Zagrebaev, Phys.Rev., C 64 (2001) 034606; V.I. Zagrebaev et al., Phys.Rev., C 65 (2002) 014607.
[6] N. Rowley, G.R. Satchler, P.H. Stelson, Phys.Lett., B **254** (1991) 25.
[7] V.I. Zagrebaev, Phys.Rev., C 67 (2003) 061601.

[8] V. Zagrebaev, V.V. Samarin and W. Greiner, Phys. Rev. C 75 (2007) 035809.
[9] L Corradi, G Pollarolo and S Szilner. J. Phys G. **36** (2009) 113101.
[10] K.Hagino, N.Rowley, A.T.Kruppa, Comp.Phys.Commun., **123** (1999) 143.
[11] V. Zagrebaev and W. Greiner, Phys. Rev. C 78 (2008) 034610.
[12] V. V. Samarin, EPJ Web of Conferences **86** (2015) 00039.
[13] A. V. Karpov, V. A. Rachkov, and V. V. Samarin, Phys. Rev. C. **92** (2015) 064603.
[14] G. I. Marchuk, *Methods of Computational Mathematics*, (Nauka, Moscow, 1980) [in Russian].